

Spiral wave chimera states in populations of oscillators mediated by a slowly varying diffusive environment

Lei Yang, Yuan He, and Bing-Wei Li*

School of Physics, Hangzhou Normal University, Hangzhou 311121, China

(Dated: June 3, 2025)

Abstract

Chimera states are usually observed in oscillator systems with nonlocal couplings. Such a nonlocal coupling arises typically as oscillators are coupled via an external environment which changes so fast that it could be eliminated adiabatically. Here we for the first time report the existence of spiral wave chimera states in large populations of Stuart-Landau oscillators coupled via a *slowly* changing diffusive environment under which the adiabatic approximation breaks down. The transition from spiral wave chimeras to spiral waves with the smooth core and to unstable spiral wave chimeras as functions of the system parameters are exploited. The phenomenological mechanism for explaining the formation of spiral wave chimeras is also proposed. The existence of spiral wave chimeras and the underlying mechanism are further confirmed in a three-component FitzHugh-Nagumo system with the similar environmental coupling scheme. Our results provide important hints to seek chimera patterns in both laboratory and realistic chemical or biological systems.

arXiv:2111.02616v1 [nlin.PS] 4 Nov 2021

* Corresponding author. Email address: bwli@hznu.edu.cn

I. INTRODUCTION

The coexistence of synchronized and desynchronized states in populations of identically coupled oscillators is known as a chimera state [1, 2]. Since its first discovery by Kuramoto and Battogtokh in 2002 [1], this counterintuitive and exotic state has inspired massive theoretical [1–14] and experimental activity [15–22]. For detailed reviews on chimera states, see Refs [23–25]. In the theoretical studies, for example, chimera states have been observed in a variety of coupled oscillator systems whose intrinsic dynamics of the element could be described by phase oscillators [1, 2], limit-cycle oscillators [7], excitable oscillators [26, 27] and chaotic maps [6]. In the experimental studies, chimera states have been realized in a spatial light modulator feedback system [15], chemical Belousov-Zhabotinsky (BZ) oscillators [16, 17], mechanically coupled metronomes [18], electrochemical systems [19, 20], electronic oscillators [21], and lasers [22], to name a few. With these studies, the conditions of generating chimera states have been broadened and generalized. Particularly, it is believed for a long time that chimera states occur only in the nonlocal coupled systems [1, 2], but recent works show that the nonlocal coupling is not necessary at all and chimera states can be observed in systems with different coupling topologies [28], including global coupling [29, 30] and local coupling [31–36]. Furthermore, the concept of chimera states has been generalized and extended largely. In addition to classical chimera states, various new types of chimera states are observed such as clustered chimeras [4], chimera death [8], amplitude-mediated chimeras [9] and amplitude chimera [8], alternating chimeras [37], traveling chimeras [38], spiral wave (scroll wave) chimeras in two (three) dimensional systems [39–41]. Besides the theoretical and experimental interests, chimera states may also have biological implications [42–45]. For example, for some birds and many mammal animals such as dolphin, one part of the brain keeps active (synchronized), while the other part of the brain remains inactive (desynchronized) when they sleep [42], which is well known as the unihemispheric slow-wave sleep (USWS). Recently, it has shown that chimera states may also exist in the human brain under some conditions such as epileptic seizures [43].

Chimera states are not only observed in one dimensional systems [1] but also in two or three dimensional systems [40, 41, 46–59]. One of the most remarkable examples in the two dimensional system is the so-called spiral wave chimera which combines the features of spiral waves and chimera states [39–41, 46–57]. Differing from the classic spiral wave whose core center is a phase singularity (or topological defect) at which the amplitude drops to zero, the core region of

the spiral wave chimera consists of a group of desynchronized oscillators running at full amplitude [39–41]. Since the first discover of such a state in the nonlocally coupled oscillator system by Kuramoto and Shima [39, 40], spiral wave chimeras have received growing interests in the last decade. In the theoretical studies, an analytical description of such a spiral wave chimera is provided by using a phase oscillator model with the nonlocal coupling, and by the perturbation method the size of the incoherent core and rotating speed could be predicted [41]. Besides periodic oscillators, spiral wave chimeras have also been reported in a complex and chaotic oscillator system [47]. It is worth mentioning that instead of nonlocally coupled systems, spiral wave chimeras are also found in locally coupled reaction-diffusion (RD) systems[50]. Recently, Totz *et al.* have verified its existence experimentally in large populations of nonlocally coupled chemical oscillators and exploited the transition from stable spiral wave chimeras to unstable ones [56].

For the aforementioned systems where chimera states are observed involving either nonlocal, local or global couplings, the interactions among oscillators are assumed to be direct. In many physical and biological oscillators, however, the individual element does not interact directly but rather by means of a common environment [60–71]. A well-known example is related to some bacteria. For them, the individual communicates with each other through signaling molecules that are released into extracellular environment, and dynamical quorum sensing (QS) occurs once the population density is beyond a critical value [60, 62, 64]. Other examples involving environmental couplings include genetic oscillators [61, 62], BZ chemical oscillators [63, 64], slime mold *Dicystelium discoideum* [65, 66], yeast cells [68], and neural oscillators [69]. Chimera states and other exotic dynamical states are reported in environmental coupling systems [72, 73].

It is often assumed that the external environment through which the individuals communicates is well-stirred [60–65]. Nevertheless, there is also a growing evidence that diffusion effects of chemical signaling molecules in the extracellular medium should be considered, which usually leads to a RD model representing a populations of oscillators coupled via a diffusive environment [66–68]. As noticed by Kuramoto and his college [40], the nonlocal coupling could be resulted from environmental coupling systems as long as the diffusive environment changes so fast that it can be eliminated adiabatically. In realistic systems such as biological systems, however, it is also quite common that the external environment may change at a rate orders of magnitude slower than their intrinsic time scale [69]. For this case, the external environment through which the oscillators coupled changes slowly compared to the oscillation of the oscillators. Under such conditions, adiabatic approximation which leads to the spatially nonlocal coupling breaks down.

As the nonlocal coupling plays a vital role in generating chimera states, an interesting question naturally arise: whether chimera states could be generated in this opposite case?

In this work, we consider a class of systems representing large populations of oscillators coupled via a slowly varying dynamical environment with diffusion. For the case of Stuart-Landau oscillators, we find that spiral wave chimeras can emerge when the time scale of the diffusive environment is much larger than that of the oscillator. Various transitions as a function of the system parameters are investigated systemically. It is found that spiral wave chimeras only occur $K < K_c$ where K denotes the coupling strength and K_c is the critical value. The mechanism underlying the emergence of spiral wave chimeras is analyzed from the point view of synchronization driven by the periodic forcing. The existence of spiral wave chimera states is further confirmed in a population of FitzHugh-Nagumo oscillators coupled through the diffusive environment which varies slowly. Our findings show that the occurrence of spiral chimera states seem robust which in turn reflects that such kind of environmentally coupled systems may be a kind of universal systems to observe them. These findings provide key hints to explore the chimera states in laboratory and realistic chemical and biological systems.

II. SPIRAL WAVE CHIMERAS IN AN ENVIRONMENTALLY COUPLED STUART-LANDAU OSCILLATOR SYSTEM

A. The Stuart-Landau oscillator model with the environmental coupling

A general model that represents a large population of oscillators coupled via a diffusive environment usually reads [66, 67, 78, 79],

$$\frac{\partial \mathbf{Z}}{\partial t} = \mathbf{F}(\mathbf{Z}) + \mathbf{H}(\mathbf{Z}, \mathbf{z}), \quad (1)$$

$$\tau \frac{\partial \mathbf{z}}{\partial t} = \mathbf{G}(\mathbf{Z}, \mathbf{z}) + \ell^2 \nabla^2 \mathbf{z}. \quad (2)$$

The column vectors $\mathbf{Z}(\mathbf{r}, t)$ and $\mathbf{z}(\mathbf{r}, t)$ represent the dynamical state of the oscillator located at the position \mathbf{r} and the external environment that the oscillator senses, respectively. The intrinsic dynamics of the oscillator is governed by $\partial_t \mathbf{Z} = \mathbf{F}(\mathbf{Z})$. The functions $\mathbf{H}(\mathbf{Z}, \mathbf{z})$ and $\mathbf{G}(\mathbf{Z}, \mathbf{z})$ are the interaction terms, which denote the effects of the environment on the oscillators and the effects of oscillators on the environment, respectively. The parameter τ represents the relative time scale of \mathbf{z} to \mathbf{Z} . In the present work, we focus on $\tau \gg 1$, which means the slow change of the environment.

The term $\ell^2 \nabla^2 \mathbf{z}$ in Eq. (2) is added to account for the diffusion of signaling molecules in the external environment.

For the specific model, we take the Stuart-Landau (SL) oscillator as the local dynamics and linear interaction between the oscillator and the environment is assumed. Explicitly, the model we are going to study could be written as

$$\frac{\partial W}{\partial t} = W - (1 + i\alpha)|W|^2W + K(S - W), \quad (3)$$

$$\tau_s \frac{\partial S}{\partial t} = W - S + \ell_s^2 \nabla^2 S. \quad (4)$$

Here $W(\mathbf{r}, t)$ is a space-time dependent complex variable representing the state of the SL oscillator and S is a complex-valued diffusive-field denoting the external environment. Compared to Eqs. (1) and (2), it is easy to find that $\mathbf{F}(W) = W - (1 + i\alpha)|W|^2W$ where α is the intrinsic frequency of the oscillator, and the interaction terms $\mathbf{H}(W, S) = K(S - W)$ and $\mathbf{G}(W, S) = W - S$ with K being the coupling strength between the oscillators and the environment. Clearly, the above system represents a large of SL oscillators coupled via a diffusive environment S . This kind of system resembles the physical model proposed to study pattern formation in the Belousov-Zhabotinsky (BZ) reaction dispersed in water droplets of a water-in-oil aerosol OT (AOT) microemulsion system (BZ-AOT system) [74] and to model spot dynamics in gas discharges [77].

Note that if the environment changes extremely fast, i.e., $\tau_s \rightarrow 0$, and then Eq. (4) can be solved using the Green function approach. Consequently, Eqs. (3) and (4) are reduced to a nonlocal coupling system which likes [39, 40]

$$\frac{\partial W}{\partial t} = W - (1 + i\alpha)|W|^2W + K \int G(\mathbf{r}', \mathbf{r})(W(\mathbf{r}', t) - W(\mathbf{r}, t))d^2\mathbf{r}', \quad (5)$$

where $G(\mathbf{r}', \mathbf{r})$ is the core of the Green function [39, 40]. The above case with the nonlocal coupling has been extensively considered in last decades. However, there is very few work on chimera states in the opposite limit, i.e., $\tau_s \gg 1$, which means the slow evolution of the environment.

B. Numerical methods and measurements

We employ the modified Euler method to solve these coupled equations with a space step $dx = dy = 0.2$ and a time step $dt = dx^2/5 = 0.008$. The system is composed of $N \times N$ grid points with $N = 1024$. To generate a spiral wave chimera, the cross-field initial conditions are used, and no-flux boundary conditions are used for the environment variable S . As we consider

the situation of the slowly changing field, we set $\tau_s = 100$. The effective diffusion constant $D_{\text{eff}} = \ell_s^2/\tau_s = 1$ for simplicity. The other parameters such as α and the coupling strength K are taken as control parameters, and we want to see how spatiotemporal dynamics, in particular how spiral wave chimeras emerges and changes as such parameters vary.

To quantify the size of the incoherent core of spiral wave chimeras through our work, we introduce an time-averaged order parameter,

$$\langle R_{j,k} \rangle = \frac{1}{2d+1} \left\langle \left| \sum_{\langle j,k \rangle} e^{i\phi_{j,k}} \right| \right\rangle \quad (6)$$

where $\phi_{j,k} = \tan^{-1}(\text{Im}W/\text{Re}W)$ denotes the oscillation phase in the complex plane of W and $\langle \cdot \rangle$ means the average over a certain time interval (e.g., $\Delta T = 5,000$ in this work). The notation $\langle j, k \rangle$ means the set of the nearest neighbor oscillators including itself and $1/(2d+1)$ is a normalization factor with d is the number of nearest oscillators along the one dimension ($d = 2$ here). From the definition of the order parameter, it is straightforward to see that for the coherent region $\langle R \rangle \approx 1$, while in the incoherent region, $\langle R \rangle$ should be less than unit. For a spiral wave chimera, we will see that there is a circular region with $\langle R \rangle < 1$ for the desynchronized core and we then could measure its diameter, d_{core} .

C. Existence and characterization of spiral wave chimeras

Figure 1 shows a typical spiral wave chimera pattern in populations of SL oscillators coupled via a slowly changing field for $K = 0.5$ and $\alpha = -0.2$. The snapshot of $\text{Re}W$ (real part of the complex variable W), the phase ϕ and its enlarged view of the core region are shown in Fig. 1(a)-(c). From these figures, one finds that oscillators in the spiral arm are phase-locked and show continuous in space, while in the circular-shaped core region they behave desynchronized in time and seem spatially discontinuous. This discontinuous property can be further demonstrated from Fig. 1 (d) showing the $\Delta\phi = \phi_{i+1, N/2} - \phi_{i, N/2}$ as a function of space along the center line. As we expect, the fluctuations of $\Delta\phi$ in the core region is quite large but almost vanishes in the region away from the core. It is also noted that most of oscillators inside the desynchronized core region oscillates much faster than that in the phase-locked arm. For example, we found that the frequency of the oscillators in the spiral arm is about 0.0046 which is much smaller than the frequency of the most central oscillator being with 0.10. Similar to the findings in three-component RD systems [50], the environment variable S with diffusion shows a normal spiral pattern, i.e., the core region

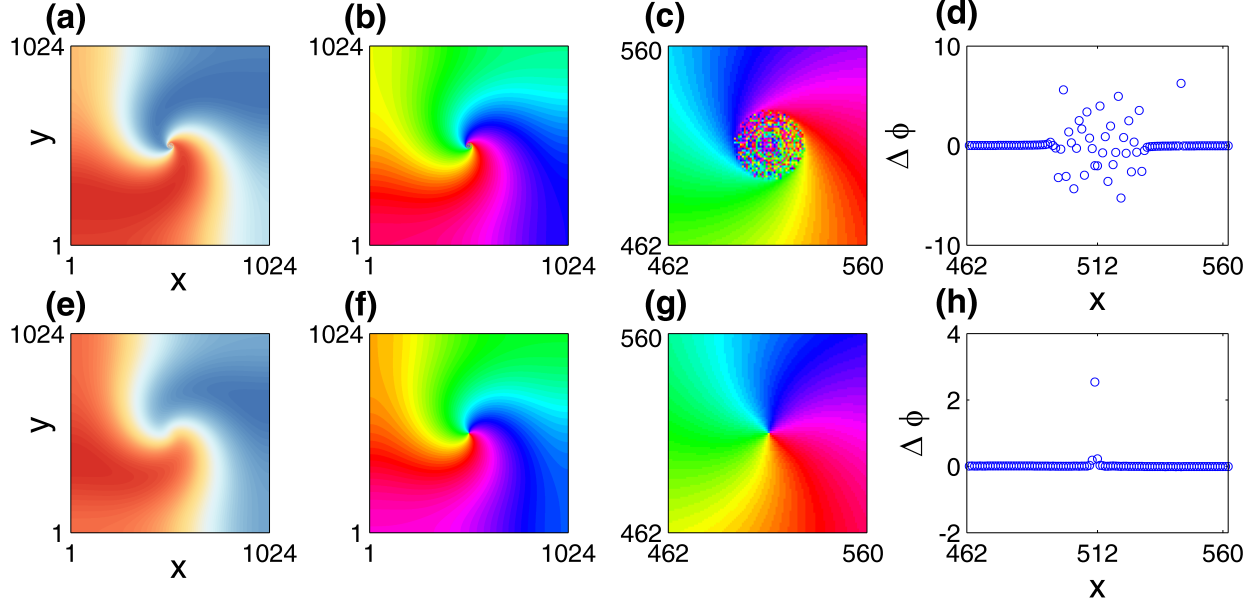


FIG. 1. (color online). Spiral wave chimeras in populations of SL oscillators coupled via a slowly changing environment. (a) A spiral wave chimera for the real component of W , and (b) the corresponding phase, i.e., ϕ , of spiral wave chimeras, and (c) enlarged view of the core region in (b). (d) The variation of $\Delta\phi = \phi_{i,N/2} - \phi_{i,N/2}$ with respect to x along the horizontal central axis in (c). (e) A spiral wave for the real component of S , and (f) the corresponding phase of spiral waves and (c) enlarged view of the core region in (f). (h) The variation of $\Delta\phi$ with respect to x along the horizontal central axis in (g). Parameters are $\alpha = -0.2$ and $K = 0.5$.

is smooth and continuous as shown in Fig. 1(e-f). Different from the component W , a well defined phase singularity can be identified which is approximately at the center of the system. It is thus that a big fluctuation only happens in the phase singularity, and except that the distribution of ϕ is smooth. This leads to a unique frequency for the environment variable S which is significantly different from W . We also note that the frequency entrainment for W and S only occurs in the spiral arm region, i.e., $\omega_{arm,W} = \omega_{arm,S}$.

The spiral wave chimera reported here is also an amplitude-mediated chimera state. That is, in addition to the phase of the oscillator, the amplitude has the chimeric feature as well. To see that clearly, we show in Fig. 2 the snapshot of $|W|$ and $|S|$, i.e., the amplitude of W and S . For $|W|$ in Fig. 2, it is found that $|W|$ is continuous and smooth outside the core region but randomized and discontinuous inside the core region. This can be further seen by plotting $\Delta|W| = |W_{i+1,N/2}| - |W_{i,N/2}|$ as a function of space as illustrated in Fig. 2(b). Similar to the

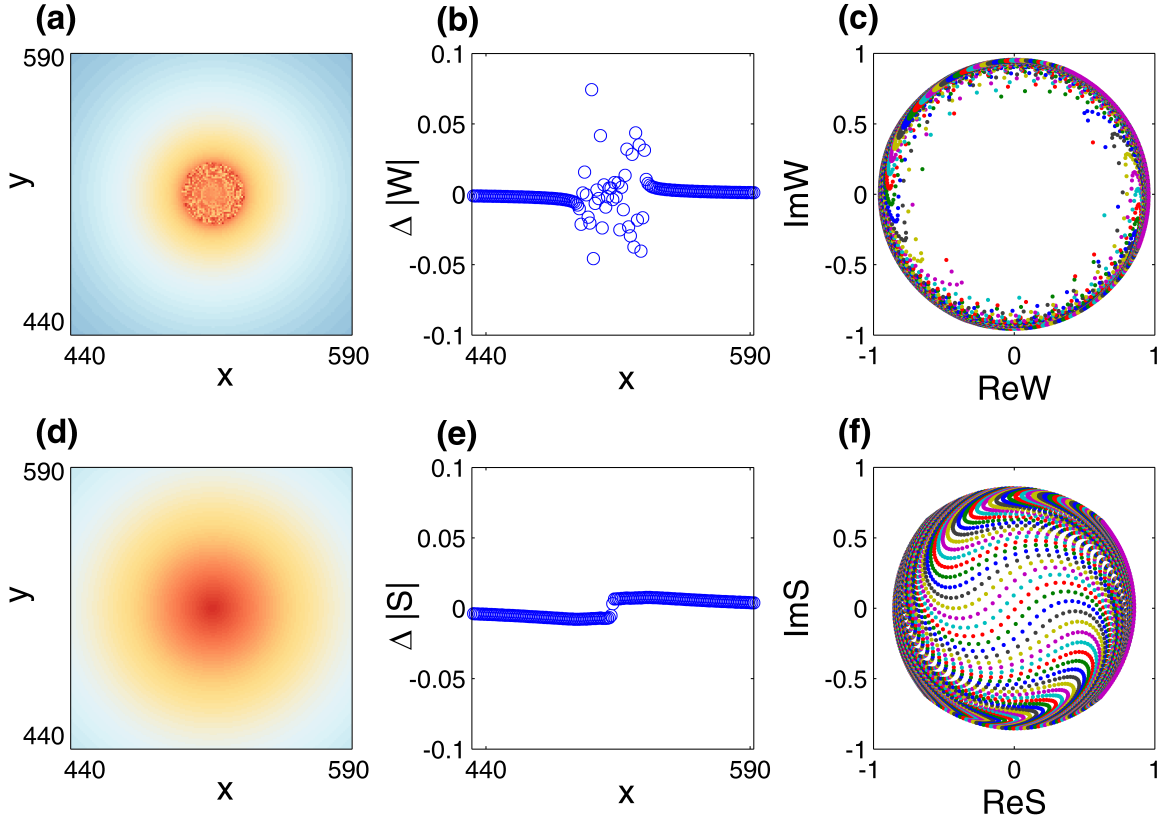


FIG. 2. (color online). The amplitude (modules) of the component of W and S and corresponding phase portraits. (a) $|W|$ near the core and (b) the variation of $\Delta|W| = |W_{i+1,N/2}| - |W_{i,N/2}|$ with respect to x along the center line. (c) The phase portrait in the $\text{Re}W - \text{Im}W$ plane. (d) $|S|$ near the core and (e) the variation of $\Delta|S| = |S_{i+1,N/2}| - |S_{i,N/2}|$ with respect to x along the center line. (f) The phase portrait in the $\text{Re}S - \text{Im}S$ plane. All the parameters are the same as in Fig.1.

phase in Fig. 1, the fluctuation is quite big inside the core but almost vanishes, i.e., $\Delta|W| \approx 0$, outside the core region. The amplitude does not drop to the zero at the core center. Instead, it has a quite large value (e.g., $|W|$ is not less than 0.65). What does it mean? It means that if we plot the states of all oscillators for any moment in the $\text{Re}W - \text{Im}W$ plane, one will see that there is a hole as illustrated in Fig. 2(c). To put it another way, the two oscillator which stays very close in the physical space may be not close at all in the state space. These features imply the discontinuous of the spatiotemporal patterns. Differing from the variable $|W|$, the amplitude of the diffusive environment variable S , i.e., $|S|$, shown in Fig. 2 (d-e) shows continuous and smooth characters. (The small gap between the left and right branch in Fig. 2(e) is due to the zero value of $|S|$ at the

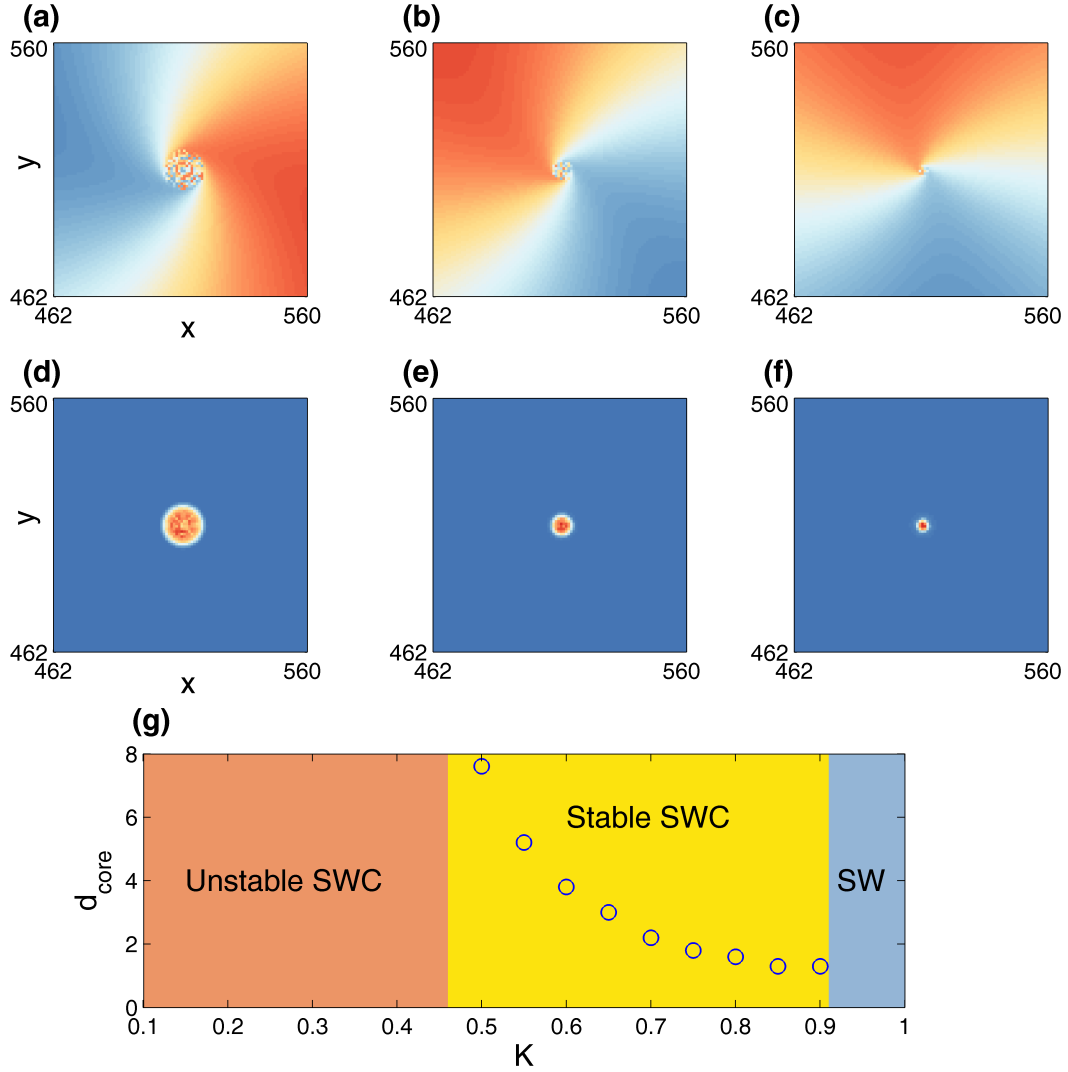


FIG. 3. (color online). The dynamical state of spiral wave chimeras as function of K . (a-c) three spiral wave chimeras for $K = 0.6, 0.7$ and 0.8 . (d-f) The averaged order parameter $\langle R \rangle$ corresponding to (a-c). (g) Regions for different dynamical states for K . The circles in this panel denote the core diameter for the corresponding coupling strength K . SWC: spiral wave chimera. SW: spiral wave. The local dynamics parameter of $\alpha = -0.2$.

phase singularity). Significantly different from Fig. 2(d), there is no hole observed in the state space expanded by $\text{Re}S - \text{Im}S$, which in turn implies that the resulted pattern of $\text{Re}S$ or $\text{Im}S$ is smooth.

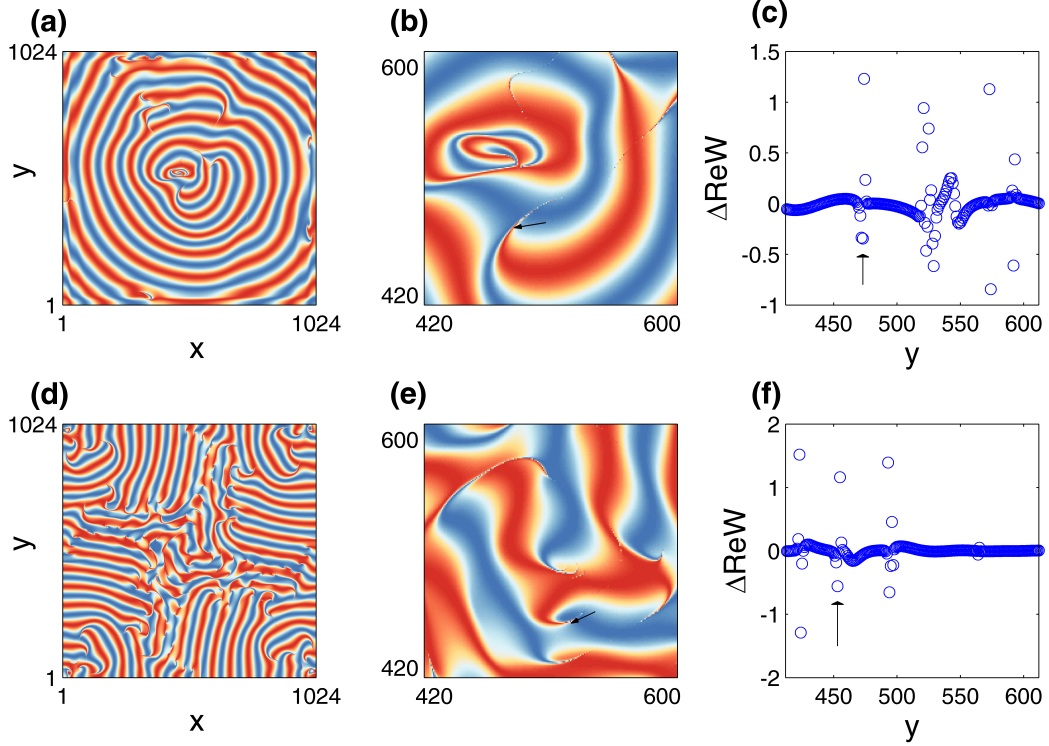


FIG. 4. (color online). Two typical states of unstable spiral wave chimeras observed in the small coupling strength K . (a) Spiral wave chimera state with core break and (b) enlarged view of the core region in (a) for $K = 0.4$. (c) The variation of $\Delta\text{Re}W = \text{Re}W_{N/2,j+1} - \text{Re}W_{N/2,j}$ with respect to y along the center line in (b). (d) A turbulent-like state and (e) enlarged view of the center region in (d) for $K = 0.2$. (f) The variation of $\Delta\text{Re}W = \text{Re}W_{N/2,j+1} - \text{Re}W_{N/2,j}$ with respect to y along the center line in (e). Other parameters are the same as in Fig. 3.

D. The effects of coupling strength K and local dynamic parameter α

In the preceding section, we have shown the existence of spiral wave chimera states in systems described by Eqs. (3-4). For this system, the parameter K determines the coupling strength between the oscillator and environment, and α represents the oscillatory frequency of the oscillator. To give more insights into the dynamics of spiral wave chimeras in this system, we try to investigate how these parameters affect the behavior of spiral wave chimeras in this section. At first, we try to identify the role played by the coupling strength in the dynamics of spiral wave chimeras. To that, we keep $\alpha = -0.2$ and vary K . Our simulations indicates that stable spiral wave chimeras are observed in a wide range of coupling strength. Figure 3 shows spiral wave chimeras and cor-

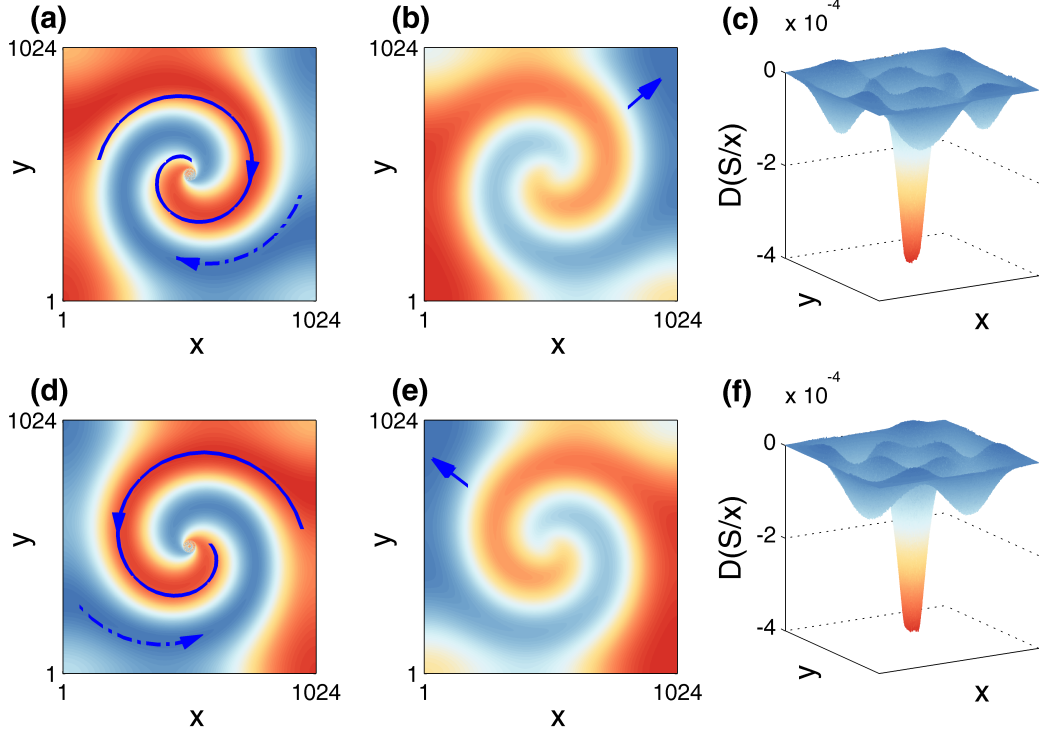


FIG. 5. (color online). The effects of α on rotation direction of spiral wave chimeras for $K = 0.65$. (a) A spiral wave chimera for ReW and (b) spiral wave for ReS rotating clockwise for $\alpha = +0.35$. (c) The spatial distribution of $D(S/x)$. (d) Spiral wave chimeras for ReW and (e) spiral wave for ReS rotating counterclockwise for $\alpha = -0.35$. (f) The spatial distribution of $D(S/x)$. The arrows with the solid (dashed) line denote the curl (rotation) direction in (a) and (d). The arrows in (b) and (e) denote the direction of wave propagation.

responding time averaged order parameter $\langle R \rangle$ for three different coupling strengths $K = 0.6, 0.7$ and 0.8 . A quantitative dependence of d_{core} on K is plotted in Fig. 3 (g). A clear fact is that the size of incoherent core, say d_{core} , decreases as coupling strength K increases and it is difficult to be distinguished between spiral wave chimeras and normal spiral waves as K tends to be unit.

Further simulations show that other dynamical states could also be observed as K varies. Specifically, for too weak coupling $K < K'_c$ where $K'_c \approx 0.46$, the spiral wave chimera is no longer stable and complex spatiotemporal patterns emerge given $\alpha = -0.2$. Figure 4 display two typical dynamical states observed in this range. In Fig. 4(a), we find the coexistence of coherent waves with several broken waves. Instead of the circular desynchronized core, each broken wave has a very slim line along which the oscillators are desynchronized (see the arrows in Fig. 4(b))

and Fig. 4(c) for example). Further decreasing K , as we find, leads to more and more broken waves and the whole patterns seems more disordered as shown in Fig. 4(d-f). It is noted that in nonlocally coupled systems, waves with such desynchronized lines have been observed [39].

The system parameter α which determines the oscillation frequency of the single oscillator would also influence the dynamics of spiral wave chimeras. Two effects are observed in our simulations. First, a transition from stable spiral wave chimera states to complex spatiotemporal patterns is observed. The resulted patterns are quite similar to those shown in Fig. 4 caused by the change of K . Second, the resulted spatial patterns are almost unchanged if we only change the sign of α , i.e., $\alpha \rightarrow -\alpha$. This is because for the isolated oscillator, changing the sign of α only alters the relative phase of $\text{Re}W$ and $\text{Im}W$. For a stable spiral wave chimera, its rotation direction reverses for the same initial condition as α changes to $-\alpha$. For instance, we show in Fig. 5 two spiral wave chimeras for $\alpha = +0.35$ and $\alpha = -0.35$, respectively. For $\alpha = +0.35$, a spiral wave chimera rotates clockwise (CW) [see the dashed arrow in Fig. 5 (a)] and waves propagate outward [see the arrow in Fig. 5(b)]; While for $\alpha = -0.35$, the spiral wave chimera rotates counterclockwise (CCW) [see the dashed arrow in Fig. 5 (d)] and waves still propagate outward [see the arrow in Fig. 5 (e)].

The reversal of the rotation direction of the spiral wave chimera is closely related to the conservation of topological charges. Specifically, once the initial condition is given, topological charges should be conserved during the evolution if there are no topological defects disappearing through the boundary. As the environment variable S is a spiral wave and its topological charge can be computed as [80]

$$\sigma = \text{sgn}[D(S/x)_{\text{PS}}]. \quad (7)$$

Here $D(S/x)$ is the z component of $\nabla S_1 \times \nabla S_2$ with $S_1 = \text{Re}S$ and $S_2 = \text{Im}S$ being the real and the imaginary part of the complex field S . That is,

$$D(S/x) = \frac{\partial S_1}{\partial x} \frac{\partial S_2}{\partial y} - \frac{\partial S_1}{\partial y} \frac{\partial S_2}{\partial x}. \quad (8)$$

For a spiral wave, $D[S/x]$ takes the maximal or minimal value at the phase singularity. Figure 5 (c) and (f) shows $D[S/x]$ for two different cases and they are almost the same as we expect. Moreover, the curl direction C [see the arrow with the solid line in Fig. 5 (a) and (d)], rotation direction R and propagation direction P satisfy following relationship as found before [80]

$$C \cdot R = P, \quad (9)$$

where $C = +1(-1)$ for CCW (CW), $R = +1(-1)$ for CCW (CW) and $P = +1(-1)$ for outward (inward) propagation.

E. Mechanism analysis

The critical coupling strength K_c below which spiral wave chimeras would arise could be estimated by the following way. As stated previously, the coupled equation represents a system among which oscillators are coupled indirectly through the diffusive environment S . The emergence of spiral wave chimeras can be viewed a continuation problem from the spiral wave solution as K changes. For $K > K_c$, the system admits the existence of a smooth core for both W and S . It is known that for this system, the value of W at the center (i.e., phase singularity) vanishes, i.e., $W(\mathbf{r}_{cent}, t) = 0$. Similarly, the value of S at the spiral center is also vanished. As K decreases to the critical value K_c , the oscillator at the spiral core center may lose its stability and become oscillatory, though the value of S at the phase singularity still vanishes. Therefore, the onset of spiral wave chimera can be regarded as the problem that the central oscillator becomes unstable for K_c due to the interaction between the oscillator and environment. In other words, to estimate K_c , we need to check the stability of the central oscillator with the environmental coupling. The equation of the central oscillator reads,

$$\frac{dW_{cent}}{dt} = W_{cent} - (1 + i\alpha)|W_{cent}|^2W_{cent} - KW_{cent}. \quad (10)$$

The above equation has a unique stationary solution $W_{cent}^{ss} = 0$. Let $\delta W = W_{cent} - W_{cent}^{ss}$, we get the evolution of the perturbation δW as,

$$\delta\dot{W} = [(1 - K) - iK\alpha]\delta W \quad (11)$$

which means the perturbation δW behaves like

$$\delta W \propto e^{(1-K-iK\alpha)t} \quad (12)$$

It immediately concludes that the stationary solution will become unstable if

$$K < K_c = 1. \quad (13)$$

This estimation is in agreement in our numerical results as illustrated in the previous section where we find the critical value of K_c is about 0.9. We note that this estimation is also true for the case of $\tau_s = 0$ as considered in the previous work [39].

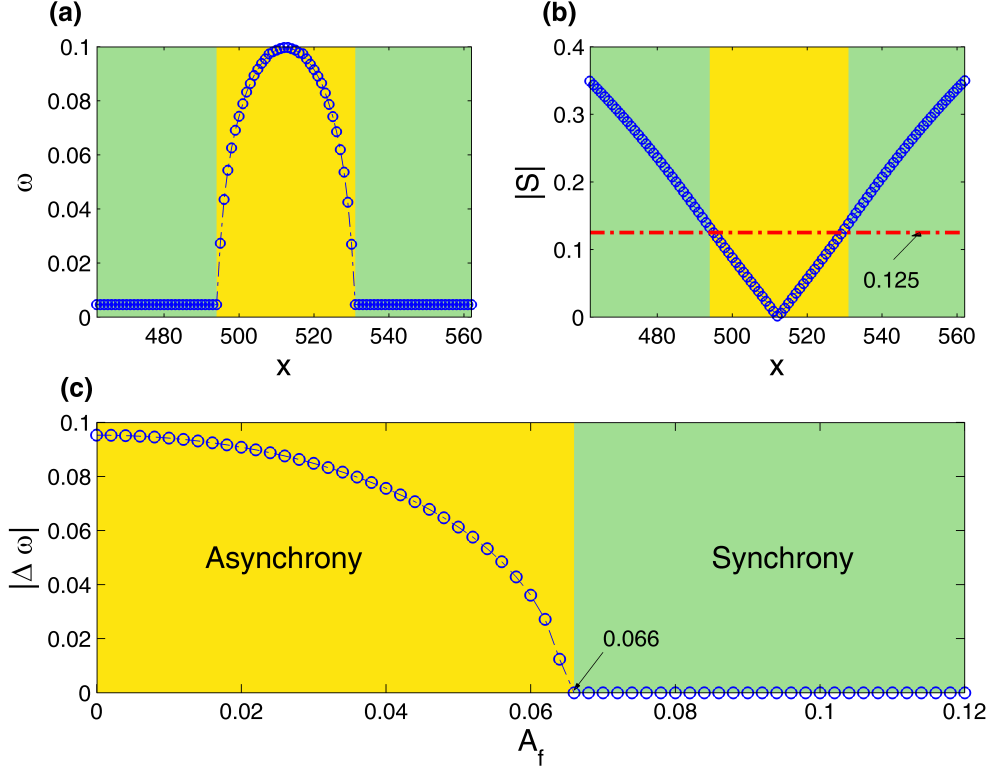


FIG. 6. (color online). Mechanism analysis of the spiral wave chimera formation. (a) Frequency profile with respect to x along the center line in Fig. 1(a). The left and right light green regions mean synchronization between W and S while the centered yellow region denotes the desynchronized. (b) $|S|$ with respect to x along the center line. (c) Frequency difference between the forcing and measured frequency, i.e., $|\Delta\omega| = |\omega_m - \omega_f|$ as a function of the forcing amplitude A_f for a local system with $\omega_f = 0.0046$. Other parameters are the same as in Fig. 1.

The formation mechanism of spiral wave chimeras in such a system can be further analyzed as follows. At first, the coupled system (3-4) can be viewed as the following picture. That is, the local oscillators are isolated from each other, but they are subjected to a spatiotemporal forcing from the environment variable S in a self-organized manner. To demonstrate this, we show an example of the central oscillator. This oscillator is absent from the forcing due to the vanished value of S at the center. Consequently, the oscillation frequency can be computed analytically by substituting $W_{cent} = \rho \exp(-i\omega t)$ into Eq. (10) and get $\omega = \alpha(1 - K)$. For the present case of $K = 0.5$ and $\alpha = -0.2$, we get $|\omega| = 0.1$ which is the same as that measured directly from the numerical simulations as illustrated in Fig. 6(a). (Please refer to the frequency of the central oscillator.)

Further rewriting Eq. (3) and denoting $F_p(t) \equiv KS_p(t)$ as the driving force for the oscillator

located at the position p , then its the dynamics is governed by

$$\frac{dW_p}{dt} = (1 - K)W_p - (1 + i\alpha)|W_p|^2W_p + F_p(t). \quad (14)$$

Please note that the driving force depends not only on time but also space. As $S_p(t)$ shows simple harmonic oscillation (no figure shown) and we then approximately replace $F_p(t)$ by a periodic forcing as $F_p(t) = A_f \exp(i\omega_f t)$ where A_f and ω_f are the amplitude and frequency of the forcing, respectively. With this approximation, the formation of spiral wave chimeras can be analyzed by a phenomenological approach with the details below. Equation (14) represents a classical situation: an oscillator subjected by a periodic forcing. According to the synchronization theory, an oscillator with the natural/intrinsic frequency ω_0 could be locked to an external periodic driving only when the frequency mismatch between them is small and the amplitude is sufficient large. Or in the other words, for a given frequency mismatch, the synchronization between the oscillator and the external forcing occurs only if the amplitude larger than a critical value, i.e., $A_f \geq A_f^c$. For the case of Fig. 1 where $K = 0.5$ and $\alpha = -0.2$, the natural frequency of the oscillator is $|\omega_0| = 0.10$. Except the phase singularity, the rotation frequency for S is the same everywhere. Therefore, we take the driven frequency ω_f as the same as the rotation frequency of spiral waves of S , i.e., $\omega_f = \omega_s = 0.0046$. With this setting, the frequency difference $\Delta\omega = |\omega_f - \omega_m|$ as a function of A_f is shown in the Fig. 6 (c). Evidently, only $A_f > A_f^c$, $\Delta\omega$ tends to be zero which means synchronization between the oscillator and external forcing occurs. For the current case, we find $A_f^c = 0.066$. This suggests that the critical amplitude of S should be $A_s^c = A_f^c/K = 0.132$. On the other hand, according to the desynchronized region in Fig. 6 and $|S|$ along the center line in Fig. 6 (b), we get the critical amplitude of S is about 0.125 (see dot lines), which is close to the predicted value $A_s^c = 0.132$ from the synchronized theory.

III. SPIRAL WAVE CHIMERAS IN A FITZHUGH-NAGUMO OSCILLATOR SYSTEM

A. The three-component FitzHugh-Nagumo model

The existence of spiral wave chimeras in populations of oscillators coupled via a slowly changing environment, as we find, is quite robust and insensitive to the specific model. To show that, we choose another kind of classical oscillator such as FitzHugh-Nagumo (FHN) type oscillator as the local dynamics of the system. Specifically, the intrinsic dynamics variables are chosen as $\mathbf{Z} = (u, v)$ and the dynamical functions as $\mathbf{F}(\mathbf{Z}) = (au - \gamma u^3 - v, u - v)$, and we set the

environmental variable $\mathbf{z} = w$. Then the interaction terms are chosen as $\mathbf{H}(\mathbf{Z}, \mathbf{z}) = -\eta w$ and $\mathbf{G}(\mathbf{Z}, \mathbf{z}) = u - w$. Finally, the coupled equations read [50, 54, 74]

$$\frac{\partial u}{\partial t} = au - \gamma u^3 - bv - \eta w, \quad (15)$$

$$\frac{\partial v}{\partial t} = u - v, \quad (16)$$

$$\tau_w \frac{\partial w}{\partial t} = u - w + l_w^2 \nabla^2 w. \quad (17)$$

Here u and v represent an activator and inhibitor, respectively. They denote the state of the oscillator. The variable w means the external environment through which oscillators communicate with each other. In one word, the above equation describes large populations of FHN oscillators coupled via a diffusive environment. As τ_w is chosen a big value, such a diffusive environment changes slowly. a , γ and b are the parameters determining the intrinsic dynamics of the oscillator. η is related to the coupling strength and l_w^2 is the diffusion coefficient of the environment variable.

We employ the explicit Euler-forward method to solve these coupled equations with a space step $dx = dy = 0.2$ and a time step $dt = dx^2/5 = 0.008$. As we consider the situation of the slowly changing field, we set $\tau_w = 100$. The effective diffusion constant $D_{\text{eff}} = \ell^2/\tau_w = 1$ for simplicity as previous. The other parameters such as $a = 4.0$, $\gamma = 4/3$, $b = 2.5$, $\eta = 3.5$ are fixed.

B. Spiral wave chimera states in FHN system

The existence of a spiral wave chimera in populations of FHN oscillators coupled via a slowly varying environment is shown in Fig. 7. Figure 7(a) and (b) display a spiral wave chimera state and its enlarged view of the core center. The rotation frequency of the spiral arm $\omega_s = 0.8569$. The difference between the adjacent oscillators $\Delta u = u_{i+1, N/2} - u_{i, N/2}$ is illustrated in Fig. 7(c) where the desynchronized region is highlighted by the yellow shaded region. Similar to the observation in the SL system, we find that the nondiffusive component u (or v) shows the feature of spiral wave chimeras and the diffusive variable w demonstrates the spiral wave with a smooth core. This facts together with previous findings strongly suggest that spiral wave chimera states in an ensemble of oscillators coupled via a slowly varying of the environment are model independent.

The underlying mechanism of the occurrence of spiral wave chimeras in the FHN coupled system can also be analyzed from the point of synchronization driven by external forcing. That is, the FHN oscillators (u, v) are subjected to a spatiotemporal forcing from the field of w . Inside the core region, the amplitude of W denoted by A_w is too weak to synchronize the FHN oscillator;

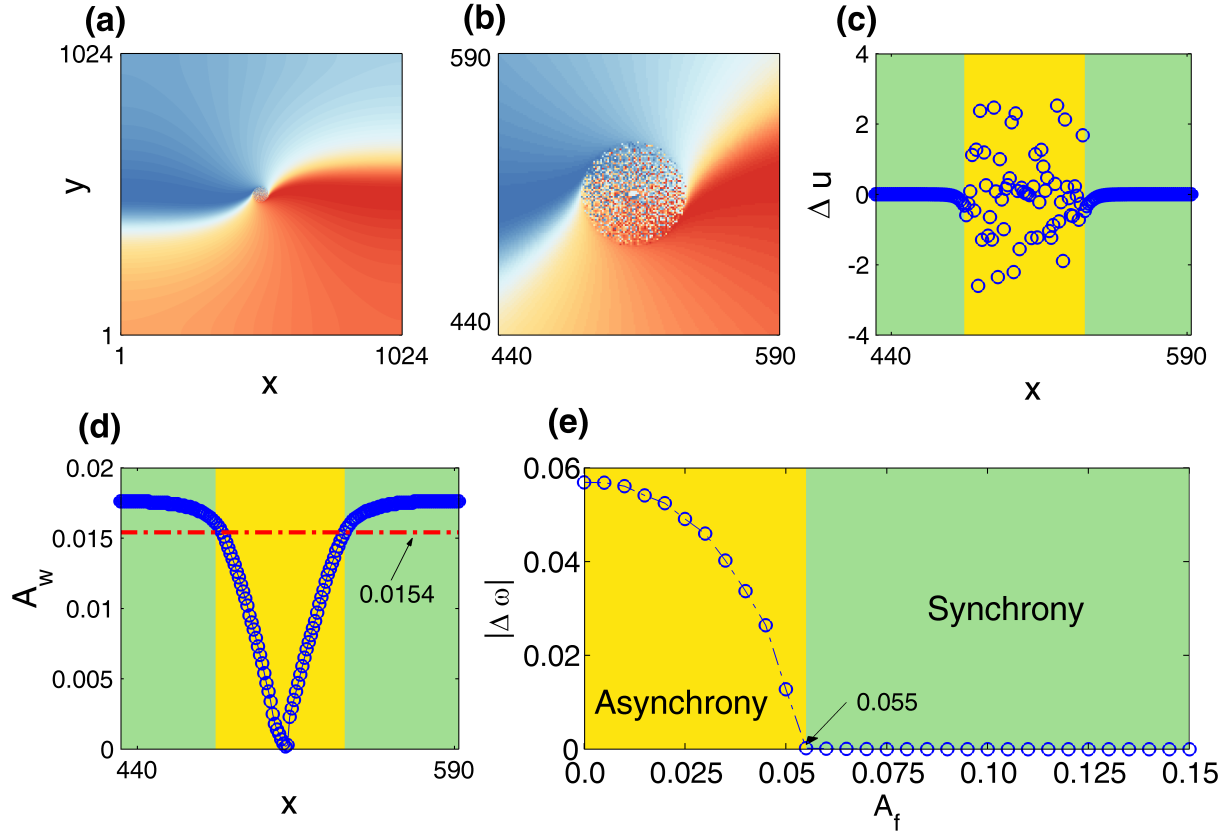


FIG. 7. (color online). Spiral wave chimeras in populations of FHN oscillators coupled via a slowly changing environment. (a) A snapshot of spiral wave chimeras for the u component and (b) enlarged view of the core region in (a). (c) The variation of $\Delta u = u_{i+1, N/2} - u_{i, N/2}$ with respect to x along the center line. (d) Time-averaged amplitude, $A_w(x)$, along central horizontal axis in (b). Frequency difference between the forcing and measured frequency, i.e., $|\Delta\omega| = |\omega_m - \omega_f|$ as a function of forcing amplitude A_f for a local system.

while outside the core, A_w is strong enough to synchronize the FHN oscillators. To illustrate that, we plot the amplitude A_w as a function of position along the center line. It is evident that inside the core, the amplitude drops to a smaller value (shading region). According to the core size, we find in this case A_w should be larger than 0.154. This critical value can be predicted by the synchronization of oscillators driven by an external forcing. Specifically, as the time evolution of

the component w like a harmonic oscillation, we then replace $-\eta w$ by $A_f \sin(\omega_f t)$, i.e.,

$$\frac{du}{dt} = au - \alpha u^3 - bv + A_f \sin(\omega_f t), \quad (18)$$

$$\frac{dv}{dt} = u - v. \quad (19)$$

For a single FHN oscillator, we get the frequency $\omega_0 = 0.812$. The driven frequency ω_f is chosen as the frequency of w and in the present case $\omega_f = \omega_s = 0.8659$. The frequency difference $\Delta\omega = |\omega_f - \omega_m|$ where ω_m is the frequency of the oscillator responded to the periodically driven as a function of A_f is illustrated in Fig. 7(e). We find that the FHN oscillator can be synchronized driven by the period forcing only if $A_f \geq A_f^c = 0.055$. This means that, the critical value of amplitude A_w^c for w should be $A_w^c = A_f^c/\eta = 0.0157$, which is well in agreement with the value 0.0154 as indicated by the dotted line in Fig. 7(d).

IV. DISCUSSION AND CONCLUSION

The environmental coupling is a quite common coupling mechanism for observations of synchrony and pattern formation in a diversity of systems ranging from physical to chemical and biological systems. In the seminal work by Kuramoto *et al.*, a key assumption to observe spiral wave chimeras is that the time scale τ of the environmental variable is so small (i.e., $\tau \rightarrow 0$) that it can be eliminated adiabatically [39, 40]. Consequently, the original system is reduced to a non-local coupled oscillator system. Laing showed that nonzero value of τ but keeping τ extremely small, chimera states could also be observed [31]. However, the question of whether chimera states could be observed in the opposite limit case, i.e., $\tau \gg 1$, is not trivial. We address this issue in this work by considering an ensemble of oscillators (SL or FHN) coupled through a slowly changing diffusive environment. We find that spiral wave chimeras could also emerge in both systems and the underlying mechanisms are similar. These important results are nontrivial extension to the previous studies of chimera states as they largely extend our knowledge and improve our understanding of the existence of the chimera state in coupled oscillator systems.

For experimentalists, there is a key question that which kinds of coupled systems are feasible to be realized in experiments. The present findings may provide some hints to this issue. Together with previous work [48, 50, 54], it shows that emergence of spiral wave chimera states is quite robust in the system representing a large populations of oscillators coupled via a diffusive field. There is a broad class of the systems with similar environmental coupling schemes such as chem-

ical oscillators BZ particles immersed in catalyst-free solutions [64], social amoeba *Dictyostelium discoideum* [66], genetically engineered bacteria [67], yeast cells [68]. Therefore, we expect that chimera states are highly possible in these biological or chemical systems. On the other hand, the realization of the nonlocal coupling in experiments up to date still strongly relies on a computer algorithm and the used system is often discretized. A main challenge in such experimental settings is to overcome the oscillator number limit. For example, realization of 10,000 chemical oscillators with the nonlocal coupling with the help of computer seems a quite difficult task in the experiment with chemical oscillators [81]. Therefore, it is not easy to extend such a two dimensional system directly to a three dimensional one where the oscillators involves much more. However, for the system presented here, the coupling is mediated by diffusion which occurs in a more natural way, and it may be easily extended to large systems and to investigate the dynamics of scroll wave chimeras in three dimension once it is realized experimentally.

In summary, by coupling a large group of oscillators to a slowly changing diffusive environment, we have shown numerically that spiral wave chimeras do exist in such systems. Given α , to observe the spiral wave chimera states, the coupling strength could not be too large or too small. As K is increased, a transition from spiral wave chimera states to spiral waves with smooth cores could occur; while K decreases and is lower than a certain critical value, spiral wave chimeras will be unstable and new kind of chimera structures could emerge. The change of α would also cause the instability and reverse the rotation of spiral wave chimeras. We further confirm that spiral wave chimera states exist in FHN systems with similar coupling schemes, which in turn suggest our findings are robust. As our system is analogy to some biological and chemical systems, the findings in the present work largely improve our understanding of the chimera state, and further provide hints to seeking chimera states in realistic systems.

ACKNOWLEDGMENTS

This work was supported by the National Natural Science Foundation of China under Grants No. 11875120 and Natural Science Foundation of Zhejiang Province under Grant No. LY16A050003.

[1] Y. Kuramoto and D. Battogtokh, Coexistence of coherence and incoherence in nonlocally coupled phase oscillators. *Nonlinear Phenom. Complex Syst.* **5**, 380 (2002).

- [2] D. M. Abrams and S. H. Strogatz, Chimera states for coupled oscillators. *Phys. Rev. Lett.* **93**, 174102 (2004).
- [3] O. E. Omel'chenko, Y. L. Maistrenko, and P. A. Tass, Chimera states: The natural link between coherence and incoherence. *Phys. Rev. Lett.* **100**, 044105 (2008).
- [4] G. C. Sethia, A. Sen, and F. M. Atay, Clustered chimera states in delay-coupled oscillator systems. *Phys. Rev. Lett.* **100**, 144102 (2008).
- [5] D. M. Abrams, R. Mirollo, S. H. Strogatz, and D. A. Wiley, Solvable model for chimera states of coupled oscillators. *Phys. Rev. Lett.* **101**, 084103 (2008).
- [6] I. Omelchenko, Y. Maistrenko, P. Hövel, and E. Schöll, Loss of coherence in dynamical networks: spatial chaos and chimera states. *Phys. Rev. Lett.* **106**, 234102 (2011).
- [7] I. Omelchenko, O. E. Omel'chenko, P. Hövel, and E. Schöll, When nonlocal coupling between oscillators becomes stronger: patched synchrony or multichimera states. *Phys. Rev. Lett.* **110**, 224101 (2013).
- [8] A. Zakharova, M. Kapeller, and E. Schöll, Chimera death: Symmetry breaking in dynamical networks. *Phys. Rev. Lett.* **112**, 154101 (2014).
- [9] G. C. Sethia, A. Sen, and G. L. Johnston, Amplitude-mediated chimera states. *Phys. Rev. E* **88**, 042917 (2013); R. Mukherjee and A. Sen, Amplitude mediated chimera states with active and inactive oscillators. *Chaos* **28**, 053109 (2018).
- [10] Y. Zhu, Z. G. Zheng, and J. Yang, Chimera states on complex networks. *Phys. Rev. E* **89**, 022914 (2014).
- [11] H. Y. Xu, G. L. Wang, L. Huang, and Y.-C. Lai, Chaos in Dirac electron optics: Emergence of a relativistic quantum chimera, *Phys. Rev. Lett.* **120**, 124101 (2018).
- [12] Y. Zhang, Z. G. Nicolaou, J. D. Hart, R. Roy, and A. E. Motter, Critical Switching in Globally Attractive Chimeras. *Phys. Rev. X* **10**, 011044 (2020).
- [13] Z. G. Zheng and Y. Zhai, Chimera state: From complex networks to spatiotemporal patterns. *Sci. Sin-Phys. Mech. Astron.* **50**, 010505 (2020).
- [14] Y. Zhang and A. E. Motter, Mechanism for Strong Chimeras. *Phys. Rev. Lett.* **126**, 094101 (2021).
- [15] A. M. Hagerstrom, T. E. Murphy, R. Roy, P. Hövel, I. Omelchenko, and E. Schöll, Experimental observation of chimeras in coupled-map lattices. *Nat. Phys.* **8**, 658 (2012).
- [16] M. R. Tinsley, S. Nkomo, and K. Showalter, Chimera and phase-cluster states in populations of coupled chemical oscillators. *Nat. Phys.* **8**, 662 (2012).

- [17] S. Nkomo, M. R. Tinsley, and K. Showalter, Chimera states in populations of nonlocally coupled chemical oscillators. *Phys. Rev. Lett.* **110**, 244102 (2013); S. Nkomo, M. R. Tinsley and K. Showalter, Chimera and chimera-like states in populations of nonlocally coupled homogeneous and heterogeneous chemical oscillators. *Chaos* **26**, 094826 (2016).
- [18] E. A. Martens, S. Thutupalli, A. Fourriere, and O. Hallatschek, Chimera states in mechanical oscillator networks. *Proc. Natl. Acad. Sci. USA* **110**, 10563 (2013).
- [19] M. Wickramasinghe and I. Z. Kiss, Spatially organized partial synchronization through the chimera mechanism in a network of electrochemical reactions. *Phys. Chem. Chem. Phys.* **16**, 18360 (2014).
- [20] L. Schmidt, K. Schönleber, K. Krischer, and V. García-Morales, Coexistence of synchrony and incoherence in oscillatory media under nonlinear global coupling. *Chaos* **24**, 013102 (2014); J. C. Wiehl, M. Patzauer and K. Krischer, Birhythmicity, intrinsic entrainment, and minimal chimeras in an electrochemical experiment. *Chaos* **31**, 091102 (2021).
- [21] L. V. Gambuzza, A. Buscarino, S. Chessa, L. Fortuna, R. Meucci, and M. Frasca, Experimental investigation of chimera states with quiescent and synchronous domains in coupled electronic oscillators. *Phys. Rev. E* **90**, 032905 (2014).
- [22] L. Larger, B. Penkovsky, and Y. Maistrenko, Laser chimeras as a paradigm for multistable patterns in complex systems. *Nat. Commun.* **6**, 7752 (2015).
- [23] M. J. Panaggio and D. M. Abrams, Chimera states: coexistence of coherence and incoherence in networks of coupled oscillators. *Nonlinearity* **28**, R67(2015).
- [24] O. E. Omel'chenko, The mathematics behind chimera states. *Nonlinearity* **31**, R121 (2018).
- [25] F. Parastesh, S. Jafari, H. Azarnoush, Z. Shahriari, Z. Wang, S. Boccaletti, and M. Perc, Chimeras. *Phys. Rep.* **898**, 1 (2021).
- [26] N. Semenova, A. Zakharova, V. Anishchenko, and E. Schöll, Coherence-resonance chimeras in a network of excitable elements. *Phys. Rev. Lett.* **117**, 014102 (2016).
- [27] Q. Dai, M. Zhang, H. Cheng, H. Li, F. Xie, and J. Yang, From collective oscillation to chimera state in a nonlocally coupled excitable system. *Nonlinear Dyn.* **91**, 1723 (2018).
- [28] B. K. Bera, S. Majhi, D. Ghosh, and M. Perc, Chimera states: Effects of different coupling topologies. *EPL* **118**, 10001 (2017).
- [29] G. C. Sethia and A. Sen, Chimera states: The existence criteria revisited. *Phys. Rev. Lett.* **112**, 144101 (2014).
- [30] A. Yeldesbay, A. Pikovsky, and M. Rosenblum, Chimeralike states in an ensemble of globally coupled

- oscillators. *Phys. Rev. Lett.* **112**, 144103 (2014).
- [31] C. R. Laing, Chimeras in networks with purely local coupling. *Phys. Rev. E* **92**, 050904(R) (2015).
- [32] M. G. Clerc, S. Coulibaly, M. A. Ferré, M. A. García-Núñez, and R. G. Rojas, Chimera-type states induced by local coupling. *Phys. Rev. E* **93**, 052204 (2016).
- [33] B. K. Bera, D. Ghosh, and T. Banerjee, Imperfect traveling chimera states induced by local synaptic gradient coupling. *Phys. Rev. E* **94**, 012215 (2016); B. K. Bera and D. Ghosh, Chimera states in purely local delay-coupled oscillators. *Phys. Rev. E* **93**, 052223 (2016).
- [34] K. Premalatha, V. K. Chandrasekar, M. Senthilvelan, and M. Lakshmanan, Stable amplitude chimera states in a network of locally coupled Stuart-Landau oscillators. *Chaos* **28**, 033110 (2018).
- [35] M. G. Clerc, S. Coulibaly, M. A. Ferré and R. G. Rojas, Chimera states in a Duffing oscillators chain coupled to nearest neighbors. *Chaos* **28**, 083126 (2018).
- [36] S. Kundu, S. Majhi, B. K. Bera, D. Ghosh, and M. Lakshmanan, Chimera states in two-dimensional networks of locally coupled oscillators. *Phys. Rev. E* **97**, 022201 (2018); S. Kundu, B. K. Bera, D. Ghosh, and M. Lakshmanan, Chimera patterns in three-dimensional locally coupled systems. *Phys. Rev. E* **99**, 022204 (2019).
- [37] S. W. Haugland, L. Schmidt, and K. Krischer, Self-organized alternating chimera states in oscillatory media. *Sci. Rep.* **5**, 9883 (2015).
- [38] J. Xie, E. Knobloch, and H.-C. Kao, Multicenter and traveling chimera states in nonlocal phase-coupled oscillators. *Phys. Rev. E* **90**, 022919 (2014).
- [39] Y. Kuramoto and S. Shima, Rotating spirals without phase singularity in reaction-diffusion systems. *Prog. Theor. Phys. Supp.* **150**, 115 (2003).
- [40] S. Shima and Y. Kuramoto, Rotating spiral waves with phase-randomized core in nonlocally coupled oscillators. *Phys. Rev. E* **69**, 036213 (2004).
- [41] E. A. Martens, C. R. Laing, and S. H. Strogatz, Solvable model of spiral wave chimeras. *Phys. Rev. Lett.* **104**, 044101 (2010).
- [42] N. C. Rattenborg, C. J. Amlaner, and S. L. Lima, Behavioral, neurophysiological and evolutionary perspectives on unihemispheric sleep. *Neurosci. Biobehav. Rev.* **24**, 817 (2000).
- [43] C. Lainscek, N. Rungratsameetaweemana, S. S. Cash and T. J. Sejnowski, Cortical chimera states predict epileptic seizures. *Chaos* **29**, 121106 (2019).
- [44] S. Majhi, B. K. Bera, D. Ghosh, and M. Perc, Chimera states in neuronal networks: A review. *Phys. Life Rev.* **28**, 100 (2019); S. Majhi, M. Perc and D. Ghosh, Chimera states in a multilayer network of

- coupled and uncoupled neurons. *Chaos* **27**, 073109 (2017).
- [45] S. Huo, C. Tian, M. Zheng, S. Guan, C. S. Zhou, and Z. Liu, Spatial multi-scaled chimera states of cerebral cortex network and its inherent structure-dynamics relationship in human brain. *Nat. Sci. Rev.* **8**, nwaa125 (2021).
- [46] C. R. Laing, The dynamics of chimera states in heterogeneous Kuramoto networks. *Physica D* **238**, 1569 (2009).
- [47] C. Gu, G. St-Yves, and J. Davidsen, Spiral wave chimeras in complex oscillatory and chaotic systems. *Phys. Rev. Lett.* **111**, 134101 (2013).
- [48] X. Tang, T. Yang, I. R. Epstein, Y. Liu, Y. Zhao, and Q. Gao, Novel type of chimera spiral waves arising from decoupling of a diffusible component. *J. Chem. Phys.* **141**, 024110 (2014)
- [49] J. Xie, E. Knobloch, and H. C. Kao, Twisted chimera states and multicore spiral chimera states on a two-dimensional torus. *Phys. Rev. E* **92**, 042921 (2015).
- [50] B. W. Li and H. Dierckx, Spiral wave chimeras in locally coupled oscillator systems. *Phys. Rev. E* **93**, 020202(R) (2016).
- [51] S. Kundu, S. Majhi, P. Muruganandam, and D. Ghosh, Diffusion induced spiral wave chimeras in ecological system. *Eur. Phys. J. Spec. Top.* **227**, 983 (2018).
- [52] S. Guo, Q. Dai, H. Cheng, H. Li, F. Xie, and J. Yang, Spiral wave chimera in two-dimensional nonlocally coupled Fitzhugh–Nagumo systems. *Chaos, Solitons, Fractals* **114**, 394 (2018).
- [53] E. Rybalova, A. Bukh, G. Strelkova, and V. Anishchenko, Spiral and target wave chimeras in a 2D lattice of map-based neuron models. *Chaos* **29**, 101104 (2019).
- [54] B. W. Li, Y. He, L. D. Li, L. Yang, and X. Wang, Spiral wave chimeras in reaction-diffusion systems: Phenomenon, mechanism and transitions. *Commun. Nonlinear Sci. Numer. Simulat.* **99**, 105830 (2021).
- [55] J. F. Tetz, M. R. Tinsley, H. Engel, and K. Showalter, Transition from spiral wave chimeras to phase cluster states. *Sci. Rep.* **10**, 7821 (2020).
- [56] J. F. Tetz, J. Rode, M. R. Tinsley, K. Showalter, and H. Engel, Spiral wave chimera states in large populations of coupled chemical oscillators. *Nat. Phys.* **14**, 282 (2018).
- [57] M. Bataille-Gonzalez, M. G. Clerc, and O. E. Omel'chenko, Moving spiral wave chimeras. *Phys. Rev. E* **104**, L022203 (2021).
- [58] B. K. Bera, S. Kundu, P. Muruganandam, D. Ghosh and M. Lakshmanan, Spiral wave chimera-like transient dynamics in three-dimensional grid of diffusive ecological systems. *Chaos* **31**, 083125

- (2021).
- [59] Y. Maistrenko, O. Sudakov, O. Osiv, and V. Maistrenko, Chimera states in three dimensions. *New J. Phys.* **17**, 073037 (2015).
 - [60] A. Camilli and B. L. Bassler, Bacterial small-molecule signaling pathways. *Science* **311**, 1113 (2006).
 - [61] J. Garcia-Ojalvo, M. B. Elowitz, and S. H. Strogatz, Modeling a synthetic multicellular clock: Re-pressilators coupled by quorum sensing. *Proc. Natl. Acad. Sci. USA* **101**, 10955 (2004).
 - [62] S. De Monte, F. d'Ovidio, S. Danø, and P. G. Sørensen, Dynamical quorum sensing: Population density encoded in cellular dynamics. *Proc. Natl. Acad. Sci. USA* **104**, 18377 (2007).
 - [63] R. Toth, A. F. Taylor, and M. R. Tinsley, Collective behavior of a population of chemically coupled oscillators. *J. Phys. Chem. B* **110**, 10170 (2006).
 - [64] A. F. Taylor, M. R. Tinsley, F. Wang, Z. Huang, and K. Showalter, Dynamical quorum sensing and synchronization in large populations of chemical oscillators. *Science* **323**, 614 (2009).
 - [65] T. Gregor, K. Fujimoto, N. Masaki, and S. Sawai, The onset of collective behavior in social Amoebae. *Science* **328**, 1021 (2010).
 - [66] J. Noorbakhsh, D. J. Schwab, A. E. Sgro, T. Gregor, and P. Mehta, Modeling oscillations and spiral waves in *Dictyostelium* populations. *Phys. Rev. E* **91**, 062711 (2015).
 - [67] T. Danino, O. Mondragón-Palomino, L. Tsimring, and J. Hasty, A synchronized quorum of genetic clocks. *Nature* **463**, 326 (2010).
 - [68] J. Schütze, T. Mair, M. J. B. Hauser, M. Falcke, and J. Wolf, Metabolic synchronization by traveling waves in yeast cell layers. *Biophys. J.* **100**, 809 (2011).
 - [69] J. J. Rubin, J. E. Rubin, and G. B. Ermentrout, Analysis of synchronization in a slowly changing environment: How slow coupling becomes fast weak coupling. *Phys. Rev. Lett.* **110**, 204101 (2013).
 - [70] J. Gou and M. J. Ward, An asymptotic analysis of a 2-D model of dynamically active compartments coupled by bulk diffusion. *J. Nonlinear Sci.* **26**, 979 (2016).
 - [71] S. A. Iyaniwura and M. J. Ward, Synchrony and oscillatory dynamics for a 2-D PDE-ODE model of diffusion-mediated communication between small signaling compartments. *SIAM J. Appl. Dyn. Syst.* **20**, 438 (2021).
 - [72] V. K. Chandrasekar, R. Gopal, D. V. Senthilkumar, and M. Lakshmanan, Phase-flip chimera induced by environmental nonlocal coupling. *Phys. Rev. E* **94**, 012208 (2016).
 - [73] C.-U. Choe, M.-H. Choe, H. Jang, and R.-S. Kim, Symmetry breakings in two populations of oscillators coupled via diffusive environments: Chimera and heterosynchrony. *Phys. Rev. E* **101**, 042213

- (2020).
- [74] S. Alonso, K. John, and M. Bär, Complex wave patterns in an effective reaction–diffusion model for chemical reactions in microemulsions. *J. Chem. Phys.* **134**, 094117 (2011).
 - [75] E. M. Nicola, M. Or-Guil, W. Wolf, and M. Bär, Drifting pattern domains in a reaction-diffusion system with nonlocal coupling. *Phys. Rev. E* **65**, 055101(R) (2002).
 - [76] A. A. Cherkashin, V. K. Vanag, and I. R. Epstein, Discontinuously propagating waves in the bathoferroin-catalyzed Belousov–Zhabotinsky reaction incorporated into a microemulsion, *J. Chem. Phys.* **128**, 204508 (2008).
 - [77] C. P. Schenk, M. Or-Guil, M. Bode, and H. G. Purwins, Interacting pulses in three-component reaction-diffusion systems on two-dimensional domains. *Phys. Rev. Lett.* **78**, 3781 (1997).
 - [78] B. W. Li, X. Z. Cao, and C. Fu, Quorum sensing in populations of spatially extended chaotic oscillators coupled indirectly via a heterogeneous environment, *J. Nonlinear Sci.* **27**, 1667 (2017).
 - [79] X. Z. Cao, Y. He, and B. W. Li, Selection of spatiotemporal patterns in arrays of spatially distributed oscillators indirectly coupled via a diffusive environment. *Chaos* **29**, 043104 (2019).
 - [80] J. T. Pan, M. C. Cai, B. W. Li, and H. Zhang, Chiralities of spiral waves and their transitions. *Phys. Rev. E* **87**, 062907 (2013).
 - [81] J. F. Tetz, *Synchronization and waves in active media*. (Springer, 2019).